PHYSICAL REVIEW D **89,** 086008 (2014)

Gauss-Bonnet correction to the *R*-current correlator in $\mathcal{N} = 4$ theory at strong coupling

Yanyan Bu*

Department of Physics, Ben-Gurion University of the Negev, Beer Sheva 84105, Israel

(Received 4 December 2013; published 11 April 2014)

We consider higher-curvature corrections to the *R*-current correlator by studying the propagation of a $U(1)$ field in Einstein–Gauss–Bonnet gravity with a negative cosmological constant. We numerically solve the Maxwell equations and plot an *R*-current spectral function with lightlike momenta, which contains pivotal information of thermal photon emission. We also analytically compute the *R*-current correlator in the long-distance limit by using the holographic membrane paradigm. In the high-energy regime, the inelastic scattering between *R*-current and gauge theory plasma is expected to happen, which will reveal the structure of the plasma at strong coupling. It turns out that the Gauss–Bonnet correction effectively rescales all physical quantities considered here by some functions of the Gauss–Bonnet coefficient. In particular, the Gauss–Bonnet terms will enhance or weaken signatures calculated here in accordance with the sign of the Gauss–Bonnet coefficient.

DOI: 10.1103/PhysRevD.89.086008 PACS numbers: 11.25.Tq, 12.38.Lg, 12.38.Mh

I. INTRODUCTION

The experimental discoveries at the Relativistic Heavy Ion Collider (RHIC) and their theoretical interpretations indicate that the hadronic matter produced after a high-energy heavy ion collision is most probably a strongly coupled ideal fluid [1,2], which should be quite different from the weakly coupled quasiparticle gas. In particular, the strong coupling nature of the quark-gluon plasma (QGP) poses a challenge for traditional methods to describe QGP: calculations based on perturbation theory of QCD are in general inappropriate. The lattice simulation can predict quantities like the hadron spectrum and thermodynamics but is still impotent in real-time dynamics due to a formidable problem of analytic continuation.

On the other hand, the discovery of gauge/gravity duality [3] provides a highly promising approach to study finite temperature large N_c gauge theory at strong coupling. Admittedly, a large N_c gauge theory is quite different and also simper than QCD. However, the results based on calculations in some large N_c gauge theories (like $\mathcal{N} = 4$ super-Yang–Mills theory) can match quite well with some QCD phenomena. Moreover, the computations using gauge/gravity duality have predicted several important results that appear to have some kind of universality among the different theories. Therefore, it is reasonable to believe that gauge/gravity is helpful in revealing some universal features of strongly coupled QGP. In the past few years, some attempts underlying gauge/gravity duality have been made toward understanding the process of heavy ion collisions as well as some properties of the strongly interacting hadronic matter; an updated review on this topic can be found in Ref. [4].

One of the most striking results as alluded to above is the shear viscosity [5] of gauge theory plasma at the strong coupling regime. In the limit of infinite 't Hooft coupling λ and infinite N_c, the ratio between shear viscosity η and entropy density s of all gauge theories with an Einstein gravity dual has been computed to the following universal value:

$$\frac{\eta}{s} = \frac{1}{4\pi}.$$

Remarkably, the smallness of this value is quite close to the one extracted from RHIC experiments. It was further conjectured in Ref. [6] that the above value is a universal lower bound for all materials. So far, all known substances including water and liquid helium satisfy the above bound.

The above ratio was obtained for a class of gauge theories for which the holographic dual is dictated by classical Einstein gravity. However, the vast string landscape tells us that string theory contains higher-derivative corrections from stringy or quantum effects, which may violate the above bound. In the gauge theory language, these effects can be thought of as the $1/\lambda$ and $1/N_c$ corrections. In Ref. [7], it was found that the leading-order $1/\lambda$ correction to η/s is positive, still consistent with the above bound. On the other hand, the $1/N_c$ correction was studied in Ref. [8] by using an effective model in gauge/gravity duality: five-dimensional Einstein–Gauss–Bonnet gravity with negative cosmological constant. The main result found there is the value of η/s for the conformal field theory dual of Gauss–Bonnet gravity, nonperturbatively in the Gauss–Bonnet coefficient α:

$$\frac{\eta}{s} = \frac{1}{4\pi}(1 - 4\alpha).$$

*yybu@post.bgu.ac.il

Therefore, when $\alpha > 0$, the Gauss–Bonnet correction will violate the bound conjectured in Ref. [6].

The shear viscosity is an important transport coefficient characterizing the hydrodynamic behaviors of the QGP. Hydrodynamics corresponds to the long-distance and long-time behavior of interacting quantum field theory around thermal equilibrium. However, if one is far away from the hydrodynamic limit, the internal structure of the QGP should be able to be probed using the analogy of deep inelastic scattering (DIS) of a high-energy lepton off a static proton. In Ref. [9], the authors considered the DIS of an R-current off $\mathcal{N} = 4$ super-Yang–Mills plasma in the limit $\lambda \to \infty$ and $N_c \to \infty$. It was claimed there that the interplay between the large N_c limit and high-energy limit turns out to be much more subtle for a single hadron target than for a plasma system. Physically, this is related to the essential feature of strong coupling nature—the deep connection between the parton distribution and unitarity of DIS. Interestingly, in the high-energy DIS regime, the dual gauge theory plasma has a partonic picture, and its structure functions were expressed in terms of the Bjorken variable x and virtuality Q^2. Shortly after this interesting work, the leading-order stringy correction $1/\lambda$ has been considered in Ref. [10]. In comparison with the infinite 't Hooft coupling result, there is an enhancement of the plasma structure functions. In Refs. [11,12], the high-energy scattering between a flavor current and holographic plasma were considered and similar results were found there.

Since the QCD plasma is expected to be optically thin, one can expect that thermal photon emitted from QGP should directly propagate without subsequent interaction. Therefore, the photon spectrum may give valuable information on properties of the QGP medium. In Ref. [13], the authors initialized the computations of the thermal photons and also dileptons emitted from finite temperature $\mathcal{N} = 4$ super-Yang–Mills gauge theory at both strong and weak coupling regimes. In the strongly coupled regime, it was found that the R-current spectral functions exhibit hydrodynamic peaks at small frequency but otherwise show no structure, like a well-defined thermal resonance, in the high temperature phase. Subsequently, this work was extended in many aspects in Refs. [14–28].

Motivated by the studies reviewed above, we here consider the Gauss–Bonnet correction to the R-current correlator in $\mathcal{N} = 4$ super-Yang–Mills plasma at the strong coupling regime. The correction modifies the correlator indirectly through the corrected metric. In this paper, we scan the parameter space of the wave vector $\{\omega, k\}$ to reveal the effect of higher-curvature corrections completely. In the hydrodynamic limit, we take holographic membrane paradigm approach [29] to perturbatively compute the R-current correlator rather than directly solving the complicated second-order differential equations. We also numerically solve the Maxwell wave equations and plot the spectral functions for the R-current. This not only checks the analytical computations in the hydrodynamic regime but also yields the photoemission rates and conductivity. Finally, in the high-energy limit, we consider the DIS of the R-current off the plasma and compute the structure functions analytically. It turns out that the Gauss–Bonnet correction will rescale all physical quantities computed above by some functions of the Gauss–Bonnet coefficient α. In particular, analogous to the work [8], the Gauss–Bonnet correction will enhance or weaken the signatures calculated in this paper according to the sign of α.

In Sec. II, we will briefly review the Gauss–Bonnet black hole geometry and also its thermodynamics. Then, we setup the gravity dual of the R-current and write down the Maxwell equations in the bulk. Section III is devoted to the numerical investigations of the R-current correlator. We will present our numerical results for the spectral functions, photoemission rates, and also the plasma conductivity in the presence of different Gauss–Bonnet corrections. In Sec. IV, we consider the Gauss–Bonnet correction to the structure functions of the gauge theory plasma dual to Einstein–Gauss–Bonnet gravity. In the Appendix, we give the hydrodynamic limit of the R-current correlator with Gauss–Bonnet corrections included to check the results presented in Sec. III.

II. HOLOGRAPHIC SETUP

A. Black hole geometry and thermodynamics

We consider a holographic model of an Einstein–Gauss–Bonnet gravity with a negative cosmological constant,

$$S_{\mathrm{GB}} = \frac{1}{2\kappa_5^2}\int d^5x\sqrt{-g}\Big[R + \frac{12}{L^2} + \frac{\alpha}{2}(R^2 - 4R_{\mu\nu}R^{\mu\nu} + R_{\mu\nu\rho\sigma}R^{\mu\nu\rho\sigma})\Big], \tag{1}$$

where α is the Gauss–Bonnet coefficient, which measures the strength of the curvature square. The above action can be roughly thought of as the gravity dual of $\mathcal{N} = 4$ super-Yang–Mills theory at strong coupling regime with inclusion of the $1/N_c$ correction.

The exact solutions and thermodynamic properties of black hole in Gauss–Bonnet gravity with the action (1) were discussed in Ref. [30]. The planar black hole solution can be written as (using the conventions of Ref. [31])

$$\begin{aligned} ds^2 &= \frac{r_0^2}{uL^2}\left(-\mathcal{A}^2 f(u)dt^2 + \sum_{i=i}^{3} dx_i^2\right) + \frac{L^2}{f(u)}\frac{du^2}{4u^2} \\ &= g_{tt}dt^2 + g_{xx}dx^2 + g_{yy}dy^2 + g_{zz}dz^2 + g_{uu}du^2, \\ f(u) &= \frac{1}{2\alpha}\left[1 - \sqrt{1 - 4\alpha(1-u^2)}\right], \quad \mathcal{A}^2 = \frac{1}{2}(1 + \sqrt{1-4\alpha}). \end{aligned} \tag{2}$$

With the above notations, the horizon is located at $u = 1$, while the asymptotic conformal boundary is at $u = 0$. The Hawking temperature, entropy density, and energy density of the black hole are

$$T = \mathcal{A}\frac{r_0}{\pi L^2}, \qquad s = \frac{1}{4G_N}\left(\frac{r_0}{L}\right)^3, \qquad \epsilon = \frac{3}{4}Ts. \quad (3)$$

It is straightforward to see that the anti-de Sitter (AdS) curvature scale of above geometry is $\mathcal{A}L$. The normalization constant $\mathcal{A}$ is chosen so that $\mathcal{A}^2 f(u=0) = 1$. In other words, the speed of light in the boundary theory is kept to unity. The causality of hydrodynamics truncated to second order in Ref. [31] will be violated unless the Gauss–Bonnet coefficient $\alpha \in [-0.711, 0.113]$. One good feature of the Gauss–Bonnet black hole lies at the exact metric form even for a finite value of α, which allows us to study the theory with finite α rather than doing expansions around $\alpha = 0$. In what follows, we will set the radius L to 1, which will simplify the expressions a little bit.

B. Dynamics of the R-current

The R-current is nothing but the conserved current associated to a gauged $U(1)$ subsector of the global $SU(4)$ R-symmetry group in $\mathcal{N} = 4$ super-Yang–Mills theory. In the language of dual gravity, its dynamics is simply dictated by the standard Maxwell term in the above asymptotically AdS black hole,

$$S = -\frac{1}{4g_5^2}\int d^5x\sqrt{-g}F_{MN}F^{MN}, \qquad \frac{1}{g_5^2} = \frac{N_c^2}{16\pi^2},$$
$$F_{MN} = \partial_M A_N - \partial_N A_M. \quad (4)$$

The classical equations of motion generated by the action (4) are the Maxwell equations in the geometry with metric (2). We will work in the radial gauge $A_u = 0$ and take a plane wave ansatz for perturbations of the residual gauge modes,

$$A_\mu(u, x_\mu) = \int \frac{d\omega dq}{(2\pi)^2} e^{-i\omega t + iqz} A_\mu(u), \qquad \mu = \{t, x, y, z\}, \quad (5)$$

where the spatial momentum is chosen to be along the third direction by using the rotational symmetry $SO(3)$ in the dual boundary theory. The bulk gauge modes $A_\mu(u)$ satisfy the $(i = x, y)$,

$$0 = \omega A_t'(u) - \frac{g^{zz}}{g^{tt}} q A_z'(u), \quad (6)$$

$$0 = A_t''(u) + [\ln(\sqrt{-g}g^{uu}g^{tt})]' A_t'(u) - \frac{g^{zz}}{g^{tt}}[q^2 A_t(u) + q\omega A_z(u)], \quad (7)$$

$$0 = A_i''(u) + [\ln(\sqrt{-g}g^{uu}g^{xx})]' A_i'(u) - \left(\frac{g^{tt}}{g^{uu}}\omega^2 + \frac{g^{zz}}{g^{uu}}q^2\right)A_i(u), \quad (8)$$

where a prime represents the derivative with respect to the holographic coordinate u.

The gauge perturbations $A_\mu(u)$ can be classified into longitudinal modes, $\{A_t(u), A_z(u)\}$, and transverse ones, $\{A_x(u), A_y(u)\}$; moreover, these two sectors are decoupled. If one differentiates Eq. (7) with respect to u and then makes use of the constraint equation (6), the dynamics of $A_t(u)$ and $A_z(u)$ can be brought into a new form,

$$0 = a''(u) + [\ln(\sqrt{-g}g^{uu}g^{uu}g^{tt}g_{zz})]' \times a'(u) + \left\{\frac{(\sqrt{-g}g^{uu}g^{tt})''}{\sqrt{-g}g^{uu}g^{tt}} - [\ln(\sqrt{-g}g^{uu}g^{tt})]' \times [\ln(\sqrt{-g}g^{zz}g^{tt})]' - \left(\frac{g^{zz}}{g^{uu}}q^2 + \frac{g^{tt}}{g^{uu}}\omega^2\right)\right\}a(u), \quad (9)$$

where we have denoted the first derivative $A_t'(u)$ as a new variable $a(u)$ to reduce the dynamical differential equation to second order. Let us further define a gauge-invariant mode $A_L(u)$ as

$$A_L(u) = A_t(u) + \frac{\omega}{q}A_z(u). \quad (10)$$

It is then direct to find an important relation between $A_L(u)$ and $a(u)$ from Eqs. (6) and (7),

$$(\sqrt{-g}g^{uu}g^{tt}a(u))' - \sqrt{-g}g^{zz}g^{tt}q^2 A_L(u) = 0. \quad (11)$$

On the other hand, one can decouple the modes $A_t(u)$ and $A_z(u)$ by writing down one dynamical equation for the gauge invariant mode $A_L(u)$:

$$\left(\frac{\sqrt{-g}g^{uu}g^{zz}q^2}{\omega^2 + q^2 g^{zz}/g^{tt}}A_L'(u)\right)' - \sqrt{-g}g^{tt}g^{zz}A_L(u) = 0. \quad (12)$$

The Minkowskian prescription proposed in the Ref. [32] to compute the finite temperature retarded Green's function of gauge-invariant operators demands us to reduce the bulk action (4) into a surface term. This will be accomplished by integrating the bulk action by parts and then making use of the Maxwell equations. In terms of the gauge-invariant mode $A_L(u)$, the surface term of the bulk action takes the following form:

$$S = -\frac{1}{2g_5^2}\int \frac{d\omega dq}{(2\pi)^2}\left\{\frac{\sqrt{-g}g^{uu}g^{zz}q^2}{\omega^2 + q^2 g^{zz}/g^{tt}}A_L(u)A_L'(u) + \sqrt{-g}g^{uu}g^{ij}A_i(u)A_j'(u)\right\}\Bigg|_{u=0}^{u=1}. \quad (13)$$

In Sec. IV, we will study the high-energy scattering and find it will be more convenient to rewrite the above on-shell action in terms of the redefined variable $a(u)$ and $A_L(u)$. After some algebraic manipulations, the bulk action reads

$$S = -\frac{1}{2g_5^2}\int \frac{d\omega dq}{(2\pi)^2}\sqrt{-g}g^{uu}\{g^{tt}A_L(u)a(u) + g^{ij}A_i(u)A_j'(u)\}|_{u=0}^{u=1}. \quad (14)$$

As a short summary of the materials presented here, we would like to state that in Sec. III and the Appendix we will mainly study Eqs. (8) and (12) and then use the on-shell action of the form (13) to study the hydrodynamic properties of the R-current correlator as well as the photoemission rates at lightlike momenta. Correspondingly, in Sec. IV, we will first change Eqs. (8) and (9) to stationary Schrödinger type and solve them using the Wentzel-Kramers-Brillouin (WKB) approximation and then use the action (14) to extract the structure functions.

III. THERMAL PHOTON EMISSION AND CONDUCTIVITY

At finite temperature, rotational symmetry plus the current conversation imply that the retarded Green's function of a conserved current J_μ (like the R-current) is completely determined up to two scalar functions: $\Pi_T(\omega, q)$ and $\Pi_L(\omega, q)$. In what follows, we will heuristically derive this conclusion by direct calculations using the dual gravity. Assume that the bulk equations of gauge perturbations $A_\mu(u)$ have already been solved. Substituting for these solutions in the on-shell action (13) and taking a second-order derivative with respect to the boundary value of $A_\mu(u)$ will yield the retarded Green's functions $G^R_{\mu\nu}$ of the R-current,

$$G^R_{LL}(\omega,q) = \frac{\sqrt{-g}g^{uu}g^{zz}q^2}{g_5^2(\omega^2+q^2g^{zz}/g^{tt})}\times\frac{A_L'(u)}{A_L(u)}\bigg|_{u=0} \sim \Pi_L(\omega,q),$$
$$G^R_{ij}(\omega,q) = \delta_{ij}\frac{\sqrt{-g}g^{uu}g^{xx}}{g_5^2}\times\frac{A_x'(u)}{A_x(u)}\bigg|_{u=0} \sim \Pi_T(\omega,q). \quad (15)$$

All the nonzero components of $G^R_{\mu\nu}(\omega, q)$ can be obtained by playing with the chain rules and will be expressed in terms of $\Pi_L(\omega, q)$ and $\Pi_T(\omega, q)$. Further discussions about the structure of $G^R_{\mu\nu}$ can be found in Ref. [33].

Generically, the bulk equations of motion cannot be solved analytically for an arbitrary choice of the wave vector $\{\omega, q\}$. In this section, we use a numerical method to solve the problem and present the results for spectral functions and photoemission rates for different Gauss–Bonnet coefficients α. In particular, the 4-momentum will be lightlike $\omega = q$ for the purposes of studying the photoemission process. In the Appendix, we also present the hydrodynamic limit of the R-current correlator as a consistent check of the numerical results of this section.

To proceed with the calculations of photoproduction from strongly coupled QGP by working with the gauge/gravity duality technique, we need some basic knowledge about thermal field theories. Consider a thermal system described by finite temperature quantum field theory. The interaction between the photon and matter can be assumed to be of the form $eJ_\mu A^\mu$, where J_μ is the electromagnetic current and e is the electromagnetic coupling constant. As in Ref. [13], the R-current will be identified as the electromagnetic current. Thermal field theory tells us that, to leading order of e, the photoemission rate from a thermal system in equilibrium is

$$d\Gamma_\gamma = \frac{d^3q}{(2\pi)^3 2\omega}e^2 n_B(\omega)\eta^{\mu\nu}\chi_{\mu\nu}(k)|_{\omega=|\vec{q}|}, \quad (16)$$

where $n_B = 1/(e^{\omega/T}-1)$ is the Bose–Einstein distribution function, $k^\mu = (\omega, \vec{q})$ the 4-momentum, and $\eta_{\mu\nu} = (-1,1,1,1)$ the Minkowski metric.

The spectral function of the current $\chi_{\mu\nu}$ is defined under the conventions

$$\chi_{\mu\nu}(k) = -2\mathrm{Im}G^R_{\mu\nu}(k),$$
$$G^R_{\mu\nu}(k) = \int d^4x e^{-ik\cdot x}\langle J_\mu(0)J_\nu(x)\rangle_T\theta(-t), \quad (17)$$

where the symbol $\langle\cdots\rangle_T$ means the expectation value in a thermal equilibrium state. In addition, the formula of ac conductivity can be obtained from the Kubo formula,

$$\sigma(\omega) = \frac{G^R_{ii}(\omega,\vec{k}=0)}{i\omega}, \quad (18)$$

where $G^R_{ii}(\omega,\vec{k}=0)$ is one spatial component of the retarded Green's function $G^R_{\mu\nu}(\omega,\vec{k}=0)$.

It was argued in Ref. [13] that the longitudinal modes make no contributions to the real photoemission. Therefore, in what follows, we only need to care about the transverse modes $A_{x/y}(u)$. Substituting for the expressions for the metric components in Eq. (8) results in

$$A_{x/y}''(u) + \frac{f'(u)}{f(u)}A_{x/y}' + \left[\frac{\tilde{\omega}^2}{uf(u)^2} - \frac{\mathcal{A}^2\tilde{q}^2}{uf(u)}\right]A_{x/y}(u) = 0, \quad (19)$$

where the dimensionless frequency and momentum are defined with respect to the temperature,

$$\tilde{\omega} = \frac{\omega}{2\pi T}, \qquad \tilde{q} = \frac{q}{2\pi T}. \quad (20)$$

We also need the explicit form of the on-shell action of transverse modes

$$S = -\frac{1}{2g_5^2}\int \frac{d\omega dq}{(2\pi)^2} 2\mathcal{A} r_0^2 f(u) \times [A_x(u)A_x'(u) + A_y(u)A_y'(u)]|_{u=0}^{u=1}. \quad (21)$$

The transverse parts of the current correlator are

$$G_{xx}^R(\omega, q) = G_{yy}^R(\omega, q) = \frac{N_c^2 T^2}{4\mathcal{A}^3} \frac{A_{x/y}'(u)}{A_{x/y}(u)}\bigg|_{u=0}. \quad (22)$$

Notice the appearance of the $\mathcal{A}$ function in the formula of the retarded Green's function. The other effect of the Gauss–Bonnet correction is contained in the dynamical equation for $A_{x/y}(u)$.

Our numerical method to solve Eq. (19) is divided into two steps. We first find the asymptotic solutions of $A_{x/y}(u)$ in the region very close to the horizon $u = 1$,

$$A_{x/y}(u) = (1-u)^{-i\tilde{\omega}/2}[1 + a_{x/y}(1-u) + b_{x/y}(1-u)^2 + c_{x/y}(1-u)^3 + \cdots], \quad (23)$$

where coefficients $a_{x/y}$, $b_{x/y}$, $c_{x/y}$, etc., are completely determined by specific choice of $\tilde{\omega}, \tilde{q}$. The factor $(1-u)^{-i\tilde{\omega}/2}$ indicates the imposition of the ingoing wave condition near the horizon. The horizon expansions presented above will be used as the initial conditions to numerically integrate the bulk equations (19) from $u = 1$ to $u = 0$.

Our numerical results are summarized as the following three plots. Recall that the value of α should be consistent with the causality requirements of holographic hydrodynamics of Gauss–Bonnet gravity, as studied in Ref. [31]. In Fig. 1 we show the trace of the spectral function with a lightlike momentum, $\chi_\mu^\mu(q = \omega)$, weighted by a factor $\mathcal{N}' = N_c^2 T^2/2$, as varying the energy of the produced photon. From different curves in Fig. 1, we can conclude that, in the hydrodynamic limit where ω/T is much smaller than unit, the spectral functions approach fixed constants for different values of α. This will be further proven by analytical calculations as presented in the Appendix. In Fig. 2, we plot the photoemission rates from the gauge theory plasma at strong coupling. The results are valid to leading order in e^2 with e the electromagnetic coupling constant but valid nonperturbatively in terms of the non-Abelian gauge coupling.

It is clear from Figs. 1 and 2 that the effect of the Gauss–Bonnet correction is nontrivial. The curves with $\alpha = 0$ correspond to the results presented in Ref. [13] for $\mathcal{N} = 4$ super-Yang–Mills theory under the limit of infinite 't Hooft coupling and infinite N_c. Inclusion of the Gauss–Bonnet correction in the bulk side will shift the curve up or down according to the sign of the coefficient α. Effectively, this can be expressed as rescaling the spectral function by some functions of α. In particular, in the infrared regime $\omega/T \ll 1$, the rescaling function is nothing but the factor $\mathcal{A}^{-1}(\alpha)$. Therefore, in the positive half-plane of α, increasing the strength of the Gauss–Bonnet correction will enhance the signal of photon emissions over the whole regime of photon frequency. Conversely, when $\alpha < 0$, the stronger the Gauss–Bonnet correction is the weaker the photon signal is. In other words, increasing the ratio η/s will decrease the differential photon emission rate, which is roughly consistent with the results obtained from hydrodynamic simulations for photon yield from QGP phase by taking into account the viscous effect as done in Ref. [34].

One intriguing observation is about the tendency of claimed rescaling function as moving into a larger ω regime. Consider the uppermost curve with $\alpha = 0.1$ in Fig. 1. With the energy of the emitted photon increased, the distance between this curve and the benchmark one with $\alpha = 0$ becomes larger, implying that the claimed rescaling function may also depend on ω. Furthermore, it seems that the effect of the Gauss–Bonnet correction is more

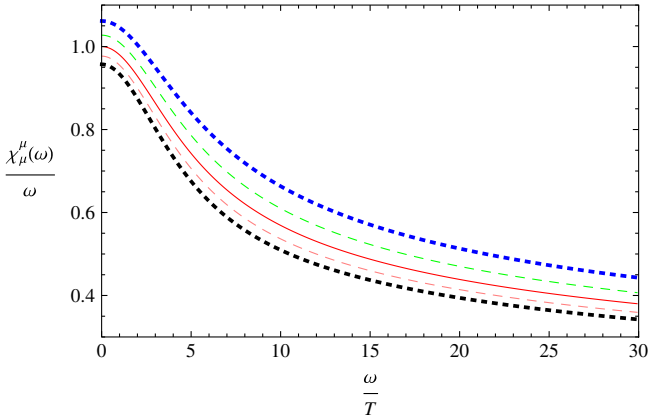

FIG. 1 (color online). Trace of the spectral function divided by frequency for lightlike momenta, $\eta^{\mu\nu}\chi_{\mu\nu}(q = \omega)/\omega$, in units of $\mathcal{N}' = N_c^2 T^2/2$. The different curves correspond to different strengths of Gauss–Bonnet corrections: $\alpha = 0.1$, 0.05, 0, −0.05, −0.1 (from top to bottom).

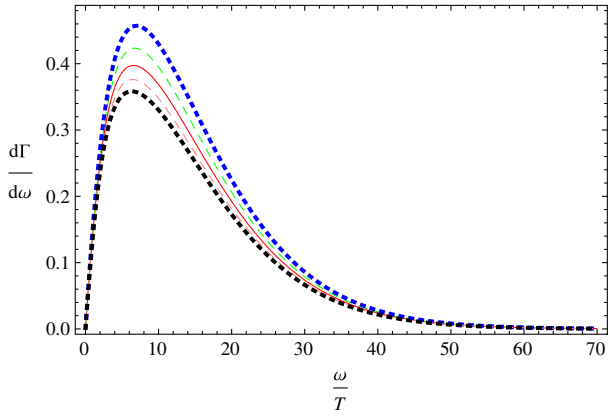

FIG. 2 (color online). Differential photoemission rate $d\Gamma_\gamma^T/d\omega$, measured with a weight function $\mathcal{N}'\frac{e^2}{4\pi}$. As in Fig. 1, different curves indicate different choices of the Gauss–Bonnet coefficient α.

important in the high-energy regime. However, when α is flipped into the negative half-plane, the effect of the Gauss–Bonnet correction is also changed. More precisely, the distance between the lowermost curve (with $\alpha = -0.1$) and the $\alpha = 0$ one of Fig. 1 in the $\omega \to 0$ is larger than its value in the large ω regime. The high-energy limit of the R-current correlator with the Gauss–Bonnet correction included will be carefully studied in Sec. IV. In comparison with the corresponding results of Ref. [9], the imaginary part of the transversal R-current correlator is rescaled by $\mathcal{A}^{-1}(1-4\alpha)^{-1/6}$. One can imagine a function $g(\alpha)$ interpolating between $\mathcal{A}^{-1}$ in the small ω regime and $\mathcal{A}^{-1}(1-4\alpha)^{-1/6}$ in the high-energy regime. These analytical investigations further prove the observation made above. Then, the imaginary part of the transversal R-current correlator can be parametrized as

$$\mathrm{Im}G^R_{ij}(\omega, q, \alpha) = g(\alpha)\mathrm{Im}G^R_{ij}(\omega, q), \tag{24}$$

where $G^R_{ij}(\omega, q)$ is the benchmark in $\mathcal{N} = 4$ super-Yang–Mills theory under the large N_c and large 't Hooft coupling limits.

In Fig. 3 we show the Gauss–Bonnet corrections to the conductivity of the dual plasma. Compared with plots in Figs. 1 and 2, there is an interesting intersection for curves with different α's around $\omega/T = 3.2$. In other words, in the low-frequency regime, positive Gauss–Bonnet coefficient will enhance the electrical conductivity; conversely, in quite large ω/T, the effect of the Gauss–Bonnet correction will be flipped. The value of dc conductivity can be obtained from the computations in the Appendix,

$$\sigma_{\mathrm{DC}} = \frac{1}{g_5^2}\Sigma_T(u)|_{u=1} = \frac{1}{\mathcal{A}}\frac{N_c^2 T}{16\pi} = \frac{\sigma_{\mathrm{DC}}(\mathcal{N}=4)}{\mathcal{A}}, \tag{25}$$

where, as alluded above, the dc conductivity is rescaled by function $\mathcal{A}$.

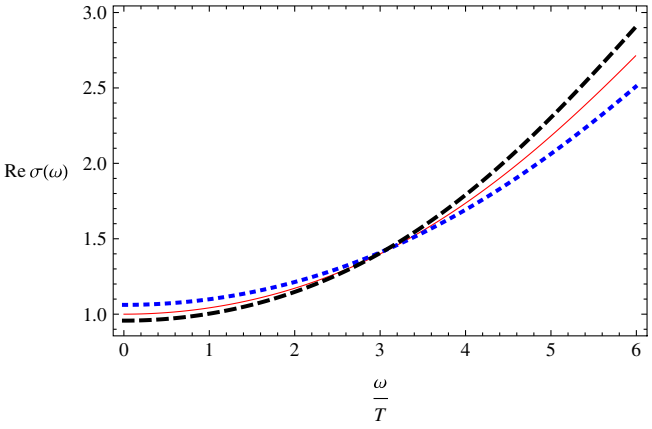

FIG. 3 (color online). Real part of the ac conductivity $\sigma(\omega)$, in units of $\mathcal{N}'$. Here, different curves are in accordance with the choices of Gauss–Bonnet coefficients $\alpha = 0.1$ (blue, dotted), 0 (red, solid), and -0.1 (black, dashed), respectively.

IV. DEEP INELASTIC SCATTERING AND STRUCTURE FUNCTIONS

A. Preliminary

The physical picture of deep inelastic scattering of a high-energy R-current off the strongly coupled QGP system was explained in great detail in Ref. [9]. We will merely recapture the materials which are most relevant to the computations presented in what follows but leave the complete understanding on this topic to the whole bulk of Ref. [9]. Roughly speaking, the process to be considered is an analog of the deep inelastic scattering between an energetic lepton and a static proton. In particular, following the general strategy of deep inelastic scattering in revealing the structure of a proton, the main work to be done is to compute the retarded correlator of the electromagnetic current $J_\mu(x)$ in a thermal equilibrium system,

$$G^R_{\mu\nu}(k) = i\int d^4x e^{-ik\cdot x}\theta(t)\langle[J_\mu(x), J_\nu(0)]\rangle, \tag{26}$$

where the current $J_\mu(x)$ will be simply taken as the R-current. This is reasonable once the R-current is weakly gauged as stated in Ref. [9]. The information on the partonic structure of a proton is totally contained in the imaginary part of $G^R_{\mu\nu}$. The expectation value is now understood as a thermal average over the ensemble of gauge theory plasma at finite temperature T. However, the fact that Eqs. (8) and (9) are second-order differential equations with real coefficients directs one to naively conclude that the structure functions are trivially zero. Anyway, the boundary condition chosen at the horizon $u = 1$ is a purely imaginary ingoing wave, which allows for a large imaginary part in the solutions of gauge modes.

The R-current conservation plus time reversal symmetry require that the retarded current correlator has the tensor structure

$$G^R_{\mu\nu}(k) = \left(\eta_{\mu\nu} - \frac{k_\mu k_\nu}{Q^2}\right)\Pi_1(x, Q^2) + \left(n_\mu - k_\mu\frac{n\cdot k}{Q^2}\right)\left(n_\nu - k_\nu\frac{n\cdot k}{Q^2}\right)\Pi_2(x, Q^2), \tag{27}$$

where n^μ is the 4-velocity of the plasma and Q^2 is the virtuality, defined as $Q^2 = q^2 - \omega^2$. We will work in the rest frame of plasma system, which means $q\cdot n = -\omega$. The DIS structure functions of the plasma are defined as

$$F_1(x, Q^2) = \frac{1}{2\pi}\mathrm{Im}\Pi_1(x, Q^2),$$
$$F_2(x, Q^2) = -\frac{q\cdot n}{2\pi T}\mathrm{Im}\Pi_2(x, Q^2), \tag{28}$$

where x represents the Bjorken variable and is defined by

$$x = -\frac{Q^2}{2(q\cdot n)T} = \frac{Q^2}{2\omega T}. \tag{29}$$

For the sake of subsequent computations, we proceed by expressing the structure functions in terms of longitudinal and transverse polarization tensors introduced in Sect. III,

$$F_1(x,Q^2) = \frac{1}{2\pi}\,\mathrm{Im}G_{ij},$$
$$F_2(x,Q^2) = \frac{\omega^2}{q^2}\left(\frac{Q^2 x}{\pi q^2}\,\mathrm{Im}G_{LL} + 2xF_1(x,Q^2)\right). \tag{30}$$

The DIS process corresponds to the large Q^2 and high-energy kinematics, where $q^2 \gg Q^2 \gg T^2$ and $\omega \simeq q$. In other words, the kinematics to be considered in this section are in the opposite corner of $\{\omega, q\}$ space as compared with the hydrodynamic limit studied in the Appendix. In addition, in what follows, we have interest only in the small x regime with $q \gg Q^2/T$, where the partonic structure of the plasma is expected. Further discussions about the parameter space in high-energy scattering between the R-current and plasma system can be found in Ref. [9].

B. Holographic computations

To get more intuition from the bulk equations, let us proceed by following Ref. [9] to rewrite Eqs. (8) and (9) as a stationary Schrödinger equation in one spatial dimension,

$$-\psi''(u) + V(u)\psi(u) = 0. \tag{31}$$

Consider the equation of longitudinal mode $a(u)$. After the introduction of a new field by $\psi_L(u) = \sqrt{uf(u)}a(u)$, Eq. (9) takes the standard time-independent Schrödinger form (31) with an effective potential $V_L(u)$ given by

$$V_L(u) = \frac{f''(u)}{2f(u)} - \frac{1}{4}\left[\frac{f'(u)}{f(u)}\right]^2 + \frac{f'(u)}{2uf(u)} - \frac{1}{4u^2} - \left\{\frac{\tilde{\omega}^2}{uf(u)^2} - \frac{\mathcal{A}^2\tilde{q}^2}{uf(u)}\right\}. \tag{32}$$

In particular, setting α to zero will go back to the results of Ref. [9],

$$V_L(u) = \frac{1}{u(1-u^2)^2}\left[-\frac{1}{4u} + \tilde{Q}^2 - \tilde{q}^2u^2\right], \tag{33}$$

where the condition $\tilde{q}^2 \gg \tilde{Q}^2 \gg 1$ has been taken into account to ignore some terms that are not important as compared to the $\tilde{Q}^2$ and $\tilde{q}^2$ ones. In addition, $\tilde{Q}^2$ denotes the the dimensionless counterpart of Q^2, i.e., $\tilde{Q}^2 = Q^2/(2\pi T)^2$.

The crucial observation made in Ref. [9] by analyzing the potential function (33) is that one can classify it into two distinct physical regimes for different ratios $\tilde{q}/\tilde{Q}^3$. Furthermore, the critical value of $\tilde{q}/\tilde{Q}^3$ corresponds to where the global maximum of the potential barrier (33) is zero. More precisely, when the parameters obey $\tilde{q}/\tilde{Q}^3 < 8/(3\sqrt{3})$, there is a high potential barrier (the global maximum of the potential is positive), with classical turning points around $u = 1/(4\tilde{Q}^2)$ and $u = \tilde{Q}/\tilde{q}$. Therefore, the wave function $\psi(u)$ is expected to be concentrated within the region $u \lesssim 1/\tilde{Q}^2$. In particular, in this regime of kinematics, the DIS structure functions should be exponentially suppressed as an imaginary part to the wave function can only develop through the quantum mechanically tunnelling effect. Conversely, when $\tilde{q}/\tilde{Q}^3 > 8/(3\sqrt{3})$ (corresponding to the high-energy limit), the potential barrier disappears. In other words, the global maximum of the potential function is negative. Then, the wave can easily move from the $u = 0$ region to the horizon $u = 1$ and is absorbed by the black hole. Therefore, a large imaginary part is expected to appear in the solution and also in the polarization tensor $G^R_{\mu\nu}$. The transverse modes can be considered in a similar fashion except for a little subtlety.

Back to the situation considered in this work, a technical obstacle comes up when repeating the above arguments. This is actually due to the good feature of the exact form of Gauss–Bonnet black hole geometry: the metric components cannot be given in the form of a finite polynomial of u. However, if α is quite small, the Gauss–Bonnet correction can be treated as a small perturbation around the large N_c and large 't Hooft limit of $\mathcal{N} = 4$ super-Yang–Mills theory. Then, the effective potential function should behave qualitatively the same as Eq. (33).[1] In particular, it is still reasonable to use the WKB technique as implemented in Ref. [35] to construct the wave function in the DIS regime. First, one finds the asymptotic solutions of Eqs. (8) and (9) near the singular points—$u = 0$ and $u = 1$, respectively. The solutions near $u = 0$ and $u = 1$ will take the form of linear combinations of some specifical functions. In the intermediate region of u, which is away from the singular points $u = 0, 1$, one can construct the WKB solutions for $\psi(u)$. Finally, the matching of the solutions together with ingoing boundary conditions at the horizon will determine the integration constants.

In the high-energy kinematics alluded to above, the effective potential $V_L(u)$ is approximated by (in the small u region)

[1]We checked the profile of $V_L(u)$ under a different choice of α within the regime consistent with the causality considerations. In particular, in the DIS regime, the Gauss–Bonnet correction makes no great modifications of $V_L(u)$'s profile even when $-0.1 \lesssim \alpha \lesssim 0.1$. Therefore, we still keep the exact forms of functions of α [like $\mathcal{A}(\alpha)$] rather than expanding them in terms of small α.

$$V_L(u) \simeq \frac{1}{u}\left[-\frac{1}{4u} + \mathcal{A}^4\tilde{Q}^2 - \frac{\mathcal{A}^6\tilde{q}^2}{\sqrt{1-4\alpha}}u^2\right]. \quad (34)$$

We can estimate the critical value of $\tilde{q}/\tilde{Q}^3$ by the inclusion of the Gauss–Bonnet correction; i.e., the maximum of the potential vanishes when $\tilde{q}/\tilde{Q}^3 = 8/(3\sqrt{3})\mathcal{A}^3 \times (1-4\alpha)^{1/4}$. If $\tilde{q}/\tilde{Q}^3$ is above this critical one, the DIS is expected to happen, and the structure functions of the plasma are not small. It was stated by the authors of Ref. [9] that the second term in the formula (34) is negligible once one considers increasing u from $u = 0$. The third term in Eq. (34) is of the same order as $1/(4u)$ around $u = 1/\tilde{q}^{2/3} \ll 1$. Therefore, $V_L(u)$ is further simplified to the following expression:

$$V_L(u) = \frac{1}{u}\left[-\frac{1}{4u} - \frac{\mathcal{A}^6\tilde{q}^2}{\sqrt{1-4\alpha}}u^2\right], \quad u \ll 1. \quad (35)$$

The general solution to the Schrödinger equation with the above potential can be constructed as a linear combination of the form

$$\psi_L(u) = c_1 J_0(\xi) + c_2 Y_0(\xi), \qquad \xi = \frac{2\mathcal{A}^3}{3(1-4\alpha)^{1/4}}\tilde{q}u^{3/2}, \quad (36)$$

where J_0 and Y_0 are the first and second kinds of Bessel functions of zeroth order, respectively. The integration constant $c_{1,2}$ can be determined by matching the small u behavior of Eq. (36) with the solutions in the intermediate regime of u. One trick to simplify the computations is the observation of Ref. [9]: in the kinematics relevant for the high-energy scattering, there is no potential barrier in $V_L(u)$. It means that the ingoing wave boundary condition required at the horizon can be equivalently imposed near the small u region.

The asymptotic expansion of solution in Eq. (36) with large variable ξ is

$$\psi_L \approx c_1\sqrt{\frac{2}{\pi\xi}}\cos\left(\xi - \frac{\pi}{4}\right) + c_2\sqrt{\frac{2}{\pi\xi}}\sin\left(\xi - \frac{\pi}{4}\right). \quad (37)$$

In particular, the ingoing wave condition can be obtained by imposing $c_1 = -ic_2$,

$$\psi_L \approx \sqrt{\frac{2}{\pi\xi}}\exp(i\xi) \Rightarrow a(u) \propto \exp[-i(\omega t - \xi)]. \quad (38)$$

The result is that, in the small u region, the solution to the longitudinal modes $a(u)$ takes the form

$$a(u) = \frac{c_1}{\sqrt{f(u)}}H_0(\xi), \quad (39)$$

where $H_0(\xi)$ is the first kind Hankel function of zeroth order. The constant c_1 will be related to the boundary value of $A_L(u)$ by the constraint equation (11),

$$c_1 = \frac{\pi}{3i}\mathcal{A}^3 A_L(0)\tilde{q}^2. \quad (40)$$

Therefore, the final expression for $a(u)$ in the small u region is

$$a(u) \approx -i\frac{\pi\tilde{q}^2}{3}\mathcal{A}^4 A_L(0)H_0(\xi), \qquad \xi = \frac{2\mathcal{A}^3}{3(1-4\alpha)^{1/4}}\tilde{q}u^{3/2}, \quad u \ll 1. \quad (41)$$

A similar analysis can be performed for the transverse modes $A_{x/y}(u)$. The new variable $\psi_T(u)$ is given by $\psi_T(u) = \sqrt{f(u)}A_{x/y}(u)$ with potential $V_T(u)$,

$$V_T(u) = \frac{f''(u)}{2f(u)} - \frac{1}{4}\left[\frac{f'(u)}{f(u)}\right]^2 - \left[\frac{\tilde{\omega}^2}{uf(u)^2} - \frac{\mathcal{A}^2\tilde{q}^2}{uf(u)}\right]. \quad (42)$$

In the small u region, $V_T(u)$ can be well approximated by the following expression:

$$V_T(u) \approx -\frac{\mathcal{A}^6}{\sqrt{1-4\alpha}}\tilde{q}^2 u, \quad u \ll 1. \quad (43)$$

Repeating the above computations, the wave function for $A_{x/y}$ with the ingoing boundary condition at horizon has the behavior in the small u region as

$$A_{x/y}(u) = \frac{\mathcal{A} \times A_{x/y}(0)}{(1-4\alpha)^{1/12}} \times \frac{i\pi}{\Gamma(1/3)}\left(\frac{\tilde{q}}{3}\right)^{1/3}\sqrt{u}H_{1/3}(\xi), \qquad \xi = \frac{2\mathcal{A}^3}{3(1-4\alpha)^{1/4}}\tilde{q}u^{3/2}, \quad u \ll 1, \quad (44)$$

where $H_{1/3}(\xi)$ is the Hankel function with order $1/3$.

With the solutions to $a(u)$ and $A_{x/y}(u)$, one can calculate the on-shell action of Eq. (14). The retarded Green's function $G^R_{\mu\nu}$, which contains the structure functions $F_{1,2}$ can be obtained from the second derivative of the on-shell action (14) with respect to the boundary values of $A_L(u)$ and $A_{x/y}(u)$. We will only list the final results for the retarded Green's functions of the R-current. In terms of longitudinal and transverse modes, their imaginary parts are given by

$$\mathrm{Im}G^R_{LL} = \frac{N_c^2T^2}{48}\pi\tilde{q}^2 \times \mathcal{A}, \qquad \mathrm{Im}G^R_{TT} = \frac{N_c^2T^2}{48}\frac{9\pi}{\Gamma(1/3)^2}\left(\frac{\tilde{q}}{3}\right)^{2/3} \times \frac{1}{\mathcal{A}(1-4\alpha)^{1/6}}. \quad (45)$$

Notice that we have expressed the final results based on those of the $\mathcal{N}=4$ super-Yang–Mills theory of Ref. [9]. Clearly, as concluded in Sec. III, the Gauss–Bonnet correction makes a rescaling of the R-current correlator even in the high-energy regime.

The structure functions are extracted from their definitions in Eq. (30) and by using the correlators (45),

$$F_1 = \frac{1}{\mathcal{A}(1-4\alpha)^{1/6}} \frac{3N_c^2T^2}{16\Gamma(1/3)^2}\left(\frac{\tilde{q}}{3}\right)^{2/3},$$
$$F_L \equiv F_2 - 2xF_1 = \mathcal{A}\frac{N_c^2Q^2x}{96\pi^2}. \tag{46}$$

These results can also be parametrized in terms of the conventional variables for DIS, x and Q^2,

$$F_T(x,Q^2) \simeq \frac{1}{\mathcal{A}(1-4\alpha)^{1/6}} \times N_c^2\frac{T^2}{x}\left(\frac{x^2Q^2}{T^2}\right)^{2/3},$$
$$F_L(x,Q^2) \simeq \mathcal{A}\times N_c^2\frac{T^2}{x}\left(\frac{x^2Q^2}{T^2}\right), \tag{47}$$

where a transverse structure function $F_T \equiv 2xF_1$ is introduced to make the final results more transparent. The symbol "≃" used in the above expressions means that we made parametric estimates of $F_{L,T}$ while ignoring the proportional factors.

Intriguingly, the longitudinal and transverse structure functions show different responses to Gauss–Bonnet corrections. In particular, if $\alpha > 0$, a Gauss–Bonnet correction will enhance the transverse structure function but suppress the longitudinal part and vice versa for the $\alpha < 0$ case. This is quite different from the $1/\lambda$ corrections considered in Ref. [10], where it was found that this stringy effect always enhances the longitudinal and transverse structure functions. Last but not least, we would like to mention that the high-energy and high-momentum limit of the transverse parts of R-current correlators (45) is quite consistent with the numerical studies made in Sec. III and also in agreement with the behaviors in hydrodynamic evaluations performed in the Appendix.

ACKNOWLEDGMENTS

The author would like to thank the hospitality of Max Planck Institute for Physics at Munich during initial stage of this work. The author has benefited much from the anonymous referee about the viscous effect on the photon emission rates. This work was supported by the Israeli Science Foundation Grant No. 87277111 and the Council for Higher Education of Israel under the PBC Program of Fellowships for Outstanding Post-doctoral Researchers from China and India (2013–2014).

APPENDIX: HYDRODYNAMIC LIMIT OF RETARDED GREEN'S FUNCTION

In this appendix, we will study the hydrodynamic limit of the R-current correlators $G^R_{\mu\nu}(\omega,q)$, which allows one to find analytical expressions for them. Roughly speaking, the hydrodynamic limit means that $\omega/T \ll 1$ and $q/T \ll 1$. Therefore, one can perturbatively solve the Maxwell equations by expanding the gauge perturbations $A_\mu(u)$ in powers of the dimensionless parameter ω/T and q/T. Within this approach, one still needs to solve second-order differential equations. Rather than solving second-order equations directly, we will take the modern form of the membrane paradigm of Ref. [29] for the purposes of revealing universality of the hydrodynamic limit in gauge/gravity computations. The materials presented here can be seen as a check of our numerical results given in Sec. III for the photoemission rates from the dual plasma.

The retarded correlator defined in Eq. (15) makes use of the linear response theory in gauge/gravity duality. At the linear level, the authors of Ref. [29] claimed another equivalent way to define the linear response function. In what follows, let us briefly summarize the main idea of Ref. [29]. First, define a canonical momentum which is conjugate to $A_\mu(u)$ with respect to a foliation in the holographic direction u,

$$\Pi_\mu(u,\omega,q) = \frac{\partial\mathcal{L}}{\partial(\partial_u A_\mu)}, \tag{A1}$$

where $\mathcal{L}$ is the Lagrangian density of the bulk action (4). The vacuum expectation value of the current dual to $A_\mu(u)$ is prescribed to be

$$\langle J_\mu(\omega,q)\rangle = \lim_{u\to 0}\Pi_\mu(u,\omega,q). \tag{A2}$$

Then, at linear level, the two-point function for the R-current $J_\mu(\omega,q)$ is given by

$$G^R{}_\mu{}^\nu(\omega,q) = \lim_{u\to 0}\frac{\Pi_\mu(u,\omega,q)}{A_\nu(u,\omega,q)}. \tag{A3}$$

One can directly show that, at the linear response level, the above definition for the two-point function is equivalent to the prescription of Ref. [32].

Relax the definition in Eq. (A3) and define a new response function at any radial surface

$$\chi(u,\omega,q) = \frac{1}{i\omega}\frac{\Pi_\mu(u,\omega,q)}{A_\nu(u,\omega,q)}. \tag{A4}$$

The dynamical equations plus the constraint one result in a first-order nonlinear equation for the response function χ. Furthermore, the ingoing boundary condition at the horizon $u=1$ is precisely the regularity condition for the

membrane paradigm. In other words, the perturbations can only depend on u and t through the Eddington–Finkelstein coordinate $v = t + u\sqrt{-g_{uu}/g_{tt}}$.

The derivation of these first-order equations obeyed by the response functions $\chi_{L/T}$ can be found in Ref. [29]. We will skip these detailed computations and just quote the main results there. Let us proceed by considering the longitudinal mode $A_L(u)$. The response function χ_L will be involved with the differential equation

$$\partial_u\chi_L = i\omega\sqrt{-\frac{g_{uu}}{g_{tt}}}\left\{\frac{\chi_L^2}{\Sigma(u)}\left(1+\frac{g^{zz}}{g^{tt}}\frac{q^2}{\omega^2}\right)-\Sigma(u)\right\} \quad \text{(A5)}$$

where the function $\Sigma(u)$ is

$$\Sigma(u) = \frac{1}{g_5^2}\sqrt{\frac{g}{g_{uu}g_{tt}}}g^{zz}. \quad \text{(A6)}$$

The longitudinal part of the retarded Green's function G^R_{LL} is

$$G^R_{LL}(\omega,q) = i\omega\lim_{u\to 0}\chi_L(u,\omega,q). \quad \text{(A7)}$$

As alluded above, the hydrodynamic limit demands that $\omega/T \ll 1$ and $q/T \ll 1$. It should be noticed that the longitudinal part of the current correlator is dictated by a pole structure in the diffusive limit $\omega \sim q^2$. Therefore, we only consider this limit for the $A_L(u)$ mode and see the Gauss–Bonnet correction to the diffusion constant. Fortunately, the diffusive limit $\omega \sim q^2$ allows us to ignore all the terms except the one proportional to q^2/ω in the right-hand side of Eq. (A5),

$$\partial_u\chi_L = \frac{iq^2}{\omega}\sqrt{-\frac{g_{uu}}{g_{tt}}}\times\frac{g^{zz}}{g^{tt}}\frac{\chi_L^2}{\Sigma(u)}, \quad \text{(A8)}$$

for which the general solution is

$$\chi_L(u,\omega,q) = \frac{1}{g_5^2}\frac{\omega\chi_L(1,\omega,q)}{\omega+iDq^2}, \quad \text{when } \frac{\omega}{T}\ll 1, \quad \frac{q}{T}\ll 1, \quad \text{and} \quad \omega^2\sim q. \quad \text{(A9)}$$

The horizon value of χ_L and the diffusion constant are

$$\chi_L(1,\omega,q) = \frac{1}{g_5^2}\sqrt{\frac{g}{g_{uu}g_{tt}}}g^{zz}\bigg|_{u=1} = \frac{1}{\mathcal{A}}\frac{N_c^2T}{16\pi},$$
$$D = \int_1^u du\sqrt{-\frac{g_{uu}g_{tt}}{g_{xx}^3}}\times g_5^2\times\chi_L(1,\omega,q) = \frac{\mathcal{A}^2}{2\pi T}(1-u). \quad \text{(A10)}$$

If the dual field theory is defined exactly at the $u = 0$ surface, it is clear that the R-charge diffusion constant surely gets correction due to the Gauss–Bonnet correction and so does the longitudinal part of the R-current correlator G^R_{LL}. In particular, in comparison with the diffusion constant of the $\mathcal{N} = 4$ super-Yang–Mills theory, the diffusion constant D now is rescaled by a function of the Gauss–Bonnet coefficient α, i.e., the $\mathcal{A}^2$ function. Moreover, the positive Gauss–Bonnet correction $\alpha > 0$ will suppress the R-charge diffusion D, and vice versa when $\alpha < 0$.

Let us turn to the transverse modes $A_{x/y}(u)$. As shown in Ref. [29], a similar differential equation can be written down for response function χ_T as in the longitudinal sector,

$$\partial_u\chi_T = i\omega\sqrt{-\frac{g_{uu}}{g_{tt}}}\left\{\frac{\chi_T^2}{\Sigma(u)}-\Sigma(u)\left(1+\frac{g^{zz}}{g^{tt}}\right)\right\}, \quad \text{(A11)}$$

where the 4-momentum is set to be lightlike $\omega = q$, which corresponds to real photoemission process considered in Sec. III. For generic frequency, the above nonlinear equation cannot be solved exactly. Therefore, we will consider the hydrodynamic limit and solve for χ_T up to the first few orders of ω. The response function χ_T can be expanded formally by powers of ω in the following way:

$$\chi_T(u,\omega) = \chi_T^{(0)} + \omega\chi_T^{(1)} + \omega^2\chi_T^{(2)} + \cdots \quad \text{(A12)}$$

The zeroth-order solution $\chi_T^{(0)}$ is trivial,

$$\partial_u\chi_T^{(0)} = 0 \Longrightarrow \chi_T^{(0)} = \Sigma(u)|_{u=1} = \frac{1}{\mathcal{A}}\frac{N_c^2T}{16\pi}, \quad \text{(A13)}$$

where we have determined the integration constant by the regularity condition at the horizon $u = 1$. We also made a convention that all the higher-order corrections $\chi_T^{(i)}(u)$ vanish exactly at the horizon $u = 1$. The zeroth-order solution for $\chi_T(u)$ can be used to extract the dc conductivity as shown in Sec. III.

The first- and second-order corrections should be solved from the following equations:

$$\partial_u\chi_T^{(1)} = i\sqrt{-\frac{g_{uu}}{g_{tt}}}\left\{\frac{\chi_T^{(0)2}}{\Sigma(u)}-\Sigma(u)\left(1+\frac{g^{zz}}{g^{tt}}\right)\right\}, \quad \text{(A14)}$$

$$\partial_u\chi_T^{(2)} = 2i\sqrt{-\frac{g_{uu}}{g_{tt}}}\frac{\chi_T^{(0)}\chi_T^{(1)}}{\Sigma(u)}. \quad \text{(A15)}$$

More higher-order corrections can be considered in similar fashion but only with more involved differential equations and will therefore be skipped here. Clearly, higher-order solutions can be obtained by direct integration with the integration constant already fixed by the vanishing condition at the horizon. The only subtlety is the appearance of divergences around the conformal boundary $u = 0$. The first-order solution is

$$\chi_T^{(1)}(u) = \frac{i}{2g_5^2\mathcal{A}}\int_1^u \left[\frac{1}{f(u)} - \frac{1}{uf(u)} + \frac{\mathcal{A}^2}{u}\right]du, \quad \text{(A16)}$$

which can be integrated to a compact form,

$$\chi_T^{(1)}(0) = \frac{N_c^2 T}{16\pi}\frac{i}{4\mathcal{A}}\left\{(\sqrt{1-4\alpha}-1)\log 2 + (1+\sqrt{1-4\alpha})\log\frac{1-4\alpha}{1-4\alpha+\sqrt{1-4\alpha}} - \sqrt{\alpha}\log\frac{1-2\sqrt{\alpha}}{1+2\sqrt{\alpha}}\right\}. \quad \text{(A17)}$$

Notice that, when $\alpha > 0$, the first-order correction $\chi_T^{(0)}(0)$ is purely imaginary and therefore makes no contributions to the R-current spectral functions. However, when $\alpha < 0$, the situation is quite different due to the last term in Eq. (A17). Because of the complicated form of the first-order correction, we will not continue with higher-order ones. Therefore, to second order in ω, the transverse part of the R-current correlator is

$$G_{TT}^R(q=\omega) = i\omega(\chi_T^{(0)}(0) + \omega\chi_T^{(1)}(0)) + \cdots, \quad \text{(A18)}$$

with $\chi_T^{(0)}(0)$ and $\chi_T^{(1)}(0)$ given above.

[1] E. Shuryak, Prog. Part. Nucl. Phys. **53**, 273 (2004).
[2] E. V. Shuryak, Nucl. Phys. **A750**, 64 (2005).
[3] O. Aharony, S. S. Gubser, J. M. Maldacena, H. Ooguri, and Y. Oz, Phys. Rep. **323**, 183 (2000).
[4] J. Casalderrey-Solana, H. Liu, D. Mateos, K. Rajagopal, and U. A. Wiedemann, arXiv:1101.0618.
[5] D. T. Son and A. O. Starinets, Annu. Rev. Nucl. Part. Sci. **57**, 95 (2007).
[6] P. Kovtun, D. Son, and A. Starinets, Phys. Rev. Lett. **94**, 111601 (2005).
[7] A. Buchel, J. T. Liu, and A. O. Starinets, Nucl. Phys. **B707**, 56 (2005).
[8] M. Brigante, H. Liu, R. C. Myers, S. Shenker, and S. Yaida, Phys. Rev. D **77**, 126006 (2008).
[9] Y. Hatta, E. Iancu, and A. Mueller, J. High Energy Phys. 01 (2008) 063.
[10] B. Hassanain and M. Schvellinger, J. High Energy Phys. 04 (2010) 012.
[11] C. B. Bayona, H. Boschi-Filho, and N. R. Braga, Phys. Rev. D **81**, 086003 (2010).
[12] Y. Y. Bu and J. M. Yang, Phys. Rev. D **84**, 106004 (2011).
[13] S. Caron-Huot, P. Kovtun, G. D. Moore, A. Starinets, and L. G. Yaffe, J. High Energy Phys. 12 (2006) 015.
[14] A. Parnachev and D. A. Sahakyan, Nucl. Phys. **B768**, 177 (2007).
[15] D. Mateos and L. Patino, J. High Energy Phys. 11 (2007) 025.
[16] A. Nata Atmaja and K. Schalm, J. High Energy Phys. 08 (2010) 124.
[17] J. Mas, J. P. Shock, J. Tarrio, and D. Zoakos, J. High Energy Phys. 09 (2008) 009.
[18] K. Jo and S.-J. Sin, Phys. Rev. D **83**, 026004 (2011).
[19] A. Rebhan and D. Steineder, J. High Energy Phys. 08 (2011) 153.
[20] B. Hassanain and M. Schvellinger, Phys. Rev. D **85**, 086007 (2012).
[21] Y. Y. Bu, Phys. Rev. D **86**, 026003 (2012).
[22] Y. Bu, Phys. Rev. D **87**, 026005 (2013).
[23] R. Baier, S. A. Stricker, O. Taanila, and A. Vuorinen, Phys. Rev. D **86**, 081901 (2012).
[24] B. Hassanain and M. Schvellinger, J. High Energy Phys. 12 (2012) 095.
[25] L. Patino and D. Trancanelli, J. High Energy Phys. 02 (2013) 154.
[26] H. -U. Yee, Phys. Rev. D **88**, 026001 (2013).
[27] S. -Y. Wu and D.-L. Yang, J. High Energy Phys. 08 (2013) 032.
[28] V. Jahnke, A. Luna, L. Patino, and D. Trancanelli, J. High Energy Phys. 01 (2014) 149.
[29] N. Iqbal and H. Liu, Phys. Rev. D **79**, 025023 (2009).
[30] R.-G. Cai, Phys. Rev. D **65**, 084014 (2002).
[31] A. Buchel and R. C. Myers, J. High Energy Phys. 08 (2009) 016.
[32] D. T. Son and A. O. Starinets, J. High Energy Phys. 09 (2002) 042.
[33] P. K. Kovtun and A. O. Starinets, Phys. Rev. D **72**, 086009 (2005).
[34] S. Sarkar, P. Roy, J. Alam, S. Raha, and B. Sinha, J. Phys. G **23**, 469 (1997).
[35] D. Teaney, Phys. Rev. D **74**, 045025 (2006).